Analysis of Validation Tests of the Langley Pilot Transonic Cryogenic Tunnel

Edward J. Ray,* Robert A. Kilgore,* Jerry B. Adcock,* and Edwin E. Davenport*
NASA Langley Research Center, Hampton, Va.

A pilot transonic cryogenic pressure tunnel has recently been developed and proof tested at the NASA Langley Research Center. In addition to providing an attractive method for obtaining high Reynolds number results at moderate aerodynamic loadings and tunnel power, this unique tunnel allows the independent determination of the effects of Reynolds number, Mach number, and dynamic pressure (aeroelasticity) on the aerodynamic characteristics of the model under test. The "proof of concept" experimental and theoretical studies are briefly reviewed. Experimental results obtained on both two- and three-dimensional models have substantiated that cryogenic test conditions can be set accurately and that cryogenic gaseous nitrogen is a valid test medium.

Nomenclature

a = local speed of sound
atm = atmospheres
c = chord of airfoil
C_N = normal force coefficient
C_P = pressure coefficient, $C_P = (P - P_\infty / q_\infty)$
C.R. = center of rotation
db = decibel
F = Fahrenheit
h = height of test section
H.P. = horsepower
ℓ = model characteristics length
L_p = sound pressure level
M = Mach number
M_ℓ = local Mach number
ΔM_ℓ = change in local Mach number
P = pressure
P_T = stagnation pressure
q = dynamic pressure, $q = \rho V^2/2$
r = radius
R = Reynolds number
R_c = Reynolds number based on chord
R/ft = Reynolds number per foot
T = temperature
T_t = stagnation temperature
v = local velocity
V = freestream velocity
x = linear dimension along airfoil chord line
z = vertical position above tunnel floor
α = angle of attack
μ = freestream viscosity
ρ = freestream density
σ = standard deviation

Subscripts

∞ = freestream
max = maximum

Introduction

FOR many years the wind tunnel has proved to be a valuable experimental device which has played an important role in the improvement of aircraft performance and flying qualities and facilitated the development of advanced aerodynamic concepts. The development of new wind tunnels has kept pace with the advances in flight Mach number capability. However, the need for substantial increases in the Reynolds number capability has become apparent in recent years, particularly at high subsonic and transonic speeds, where shock boundary-layer interactions and other viscous effects can have unusally large effects on stability and performance characteristics. In this regard, it is generally accepted that the capability should exist for minimum test Reynolds numbers, based on the mean aerodynamic chord, on the order of 50×10^6. The above goal represents an increase in Reynolds number capability by about a factor of 5 over that of existing transonic tunnels in the United States.

Although the necessity for transonic wind tunnels capable of achieving high Reynolds numbers has been recognized by researchers for many years, the problems imposed by economics and lack of technology have until recently made it impractical to construct a facility of this type. Nevertheless, design approaches to achieve high test Reynolds numbers have been the subject of intense studies for a number of years. One of the most innovative concepts to surface was to operate wind tunnels at cryogenic temperatures. This concept was first proposed by Smelt[1] in 1945 as an attractive method for achieving high test Reynolds numbers at reasonable levels of drive power in fan-driven tunnels. However, at the time of Smelt's work, the lack of a practical means of cooling a wind tunnel to cryogenic temperatures and the unavailability of suitable structural materials precluded the application of the cryogenic wind-tunnel concept. During the latter part of 1971, a study was begun at the Langley Research Center to determine the feasibility of applying the cryogenic concept to a high Reynolds number transonic wind tunnel. The analyses of Smelt were extended and a small low-speed model tunnel was modified for cryogenic operation.[2] Results obtained from these initial studies stimulated the design and construction of the Langley pilot transonic cryogenic tunnel. This tunnel was placed in operation in Sept. 1973 and some of the initial results obtained were reported in Ref. 3. As a result of the successful operation during the validation studies, the pilot cryogenic tunnel has been reclassified by NASA as a research facility and as such is being used for aerodynamic research as well as cryogenic technology studies. The purpose of this paper is to provide a brief review of the cryogenic concept and to present an analysis of some of the recent experimental results obtained in the Langley pilot cryogenic tunnel.

Why Cryogenics?

There are several approaches which will provide the desired increase in Reynolds number capability. Reynolds number,

Presented as Paper 74-631 at the AIAA 8th Aerodynamics Testing Conference, Bethesda, Maryland, July 8-10, 1974; submitted July 22, 1974; revision received December 20, 1974.

Index categories: Research Facilities and Instrumentation; Subsonic and Transonic Flow; Aircraft (Including Component Wind-Tunnel Testing).

*Aerospace Engineer, Subsonic-Transonic Aerodynamics Division. Member AIAA.

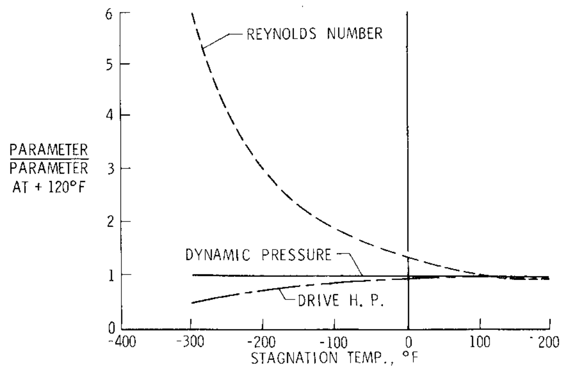

Fig. 1 Some effects of cryogenic operation. $M_\infty = 1.0$, $P_T = 1$ atm.

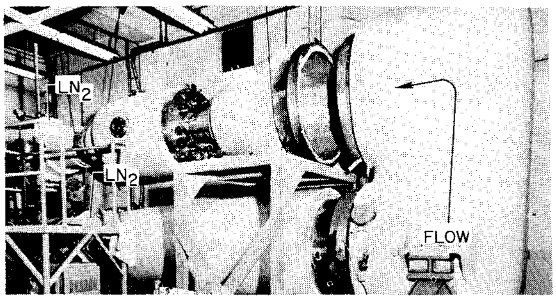

Fig. 2 Photograph of Langley pilot transonic cryogenic tunnel during initial assembly.

the ratio of the inertia forces to the viscous forces, is given by

$$R = (\rho V^2 \ell^2 / \mu V \ell) \tag{1a}$$

which reduces to the well-known equations

$$R = (\rho V \ell / \mu) \tag{1b}$$

or

$$R = (\rho M a \ell / \mu) \tag{1c}$$

From the equation for Reynolds number, an obvious way to increase Reynolds number is to increase the model size, that is, increased ℓ. For constant wall interference this method requires a commensurate increase in wind-tunnel size which results in excessively large, costly facilities with prohibitive power requirements. An alternate solution is to restrict the tunnel and model sizes and increase the operating pressure and, consequently, the density ρ. This method is feasible, of course, but the aerodynamic forces on the model, balance, and support system are greatly increased at the operating pressures that would be required to achieve the desired Reynolds number. From a power standpoint, a high-pressure tunnel is preferable to the large, moderate pressure tunnel. However, for the required increase in Reynolds number, the power requirements are still undesirably large. A third method for increasing Reynolds number is to decrease the temperature of the test gas. As temperature is reduced, the density ρ increases, the viscosity μ decreases, and the speed of sound a decreases. While the benefits of these effects of cryogenic operation are readily apparent from the usual forms of the Reynolds number equation [Eqs. (1b) or (1c)], it is informative to inspect the inertia and viscous forces separately in Eq. (1a). It thus can be shown that the increase in density and decrease in velocity (for a given M) cancel such that there is no change in the inertia force and that there is a large decrease in the viscous force due both to the decreasing viscosity and decreasing velocity. The result is a large increase in Reynolds number without the large increase in inertia or dynamic pressure that accompanies the pressure tunnel approach. In addition, the reduced velocity results in large reduction in drive power requirements and energy consumption.[3]

Figure 1 provides some insight into the magnitude of the advantages of testing at cryogenic temperatures. The ratios of several key test parameters to their values at a typical ambient temperature condition are plotted against stagnation temperature. It can readily be seen that at cryogenic temperatures the Reynolds number is increased by a factor of about 6 with no increase in dynamic pressure and with a reduction of about half in the required drive power. There are, in addition, some important advantages with respect to the kinds of testing possible in a tunnel capable of cryogenic operation. As noted in Ref. 3, with the unique ability to control tunnel temperature, pressure, and Mach number separately, it is possible to determine independently the effects of Reynolds number, dynamic pressure, and compressibility on the aerodynamic characteristics of the model under test. Because of the many inherent advantages associated with testing at low temperatures, the cryogenic approach appears to be the most desirable method for acquiring transonic test results at high Reynolds number.

Langley Pilot Transonic Cryogenic Tunnel

The Langley pilot transonic cryogenic tunnel is a continuous flow, fan driven facility with a slotted octagonal test section 13.5 in. across the flats. A photograph of the cryogenic tunnel during initial assembly is shown in Fig. 2. From the vantage shown in Fig. 2, the fan is positioned in the lower left-hand corner of the tunnel circuit and the flow is counterclockwise.

The tunnel is constructed of aluminum alloy and is encased in thermal insulation consisting of about 5 in. of urethane foam covered with a fiberglass reinforced epoxy vapor barrier. The fan is driven by a 3000 H.P. variable-frequency motor. The Mach number of the cryogenic tunnel can be varied from about 0.05-1.2 at stagnation pressures varying from about 1-5 atm. The tunnel temperatures can be reduced to about -320° F by spraying liquid nitrogen directly into the tunnel circuit at two points, located just before the upper left-hand and just after the lower left-hand turns shown in the photograph of Fig. 2. Viewing ports of 1.4-in. diam are provided for monitoring the test section and the nitrogen injection zones.

Since this tunnel was to be the first transonic cryogenic tunnel in existence and was in itself a proof-of-concept vehicle, a rather extensive amount of instrumentation was incorporated in the design. The installed instrumentation allows measurements to be made of: about 100 static pressures, 4 stagnation pressures, 30 temperatures, noise, dew point, and oxygen content of the test gas, liquid nitrogen flow rate, exhaust mass flow rate, drive-shaft torque, and fan speed. In addition to the "permanently" installed devices, the instrumentation included pressure and temperature rakes for evaluating vertical, lateral, and horizontal pressure and temperature distributions in the test section.

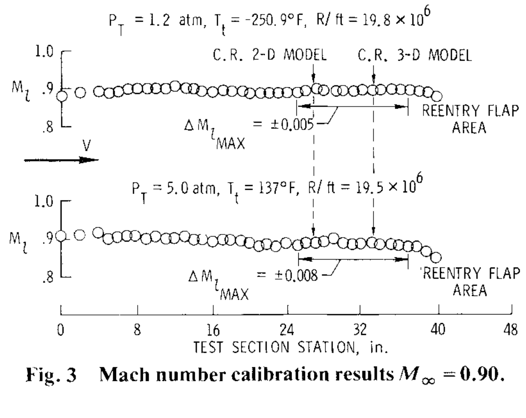

Fig. 3 Mach number calibration results $M_\infty = 0.90$.

Proof-of-Concept Studies

Mach Number Calibration

An extensive series of calibrations were conducted to determine the Mach number distribution in the test section. The operating envelope was covered in detail with special attention given to obtaining comparisons which would indicate any disparities that might occur between results at ambient and at cryogenic temperatures. The calibrations were made with a 3/4-in. diam center line pressure probe which surveyed about 40 in. of the test section. Figure 3 presents a sample of the results which were obtained for two different test conditions. The results shown in the upper portion of the figure shows the local Mach number M_ℓ distribution in the test section at a stagnation pressure of 1.2 atm and a cryogenic temperature of about $-251°$F. The Mach number distribution shown in the lower portion of Fig. 3 was recorded at a stagnation pressure of 5 atm and a temperature of 137°F. In both cases the flow similarity parameters were almost identical; the freestream Mach number was 0.90, and the Reynolds number was about 20×10^6 per ft. In Fig. 3 center of rotation C.R. stations are indicated for two different models. (The two-dimensional and three-dimensional model studies are discussed in subsequent sections of this paper.) For the indicated test region, the maximum "scatter" in the local Mach number was about 0.008. Also, there is a marked similarity between the two calibrations, and in both cases there is about 20-30 in. of "good" flow upstream of the model. These results are typical of the high subsonic calibrations which were obtained. The deviation in Mach number was considerably less at the low Mach numbers but was increased at the higher Mach numbers, with shorter regions of "good" flow. It should be noted, however, that at this time no attempt has been made to optimize the test-section geometry to improve the flow characteristics at the higher Mach numbers.

Temperature Distribution Calibrations

As previously mentioned, the wide range of operating temperatures is obtained by spraying liquid nitrogen directly into the tunnel circuit to cool the structure and test gas and to remove the heat added to the stream by the drive fan. Because of this method of cooling, the uniformity of the temperature distribution was one of the areas of concern at the beginning of the cryogenic studies at Langley. To determine the extent of the mixing process and to evaluate the temperature distributions, a temperature survey ring was placed just upstream of the screens in the tunnel. A photograph of the survey ring is shown in Fig. 4.

The ring incorporated 24 thermocouples which were evenly spaced along 8 spokes 45° apart. The screen section was located just downstream of the turn in the tunnel circuit shown in the upper right-hand portion of Fig. 2.

Figure 5 indicates typical examples of the distributions which were determined with the temperature survey ring. These particular samples were obtained at a test-section Mach number of 0.85 and a stagnation pressure of 5 atm. The data shown at the left were obtained when the tunnel stagnation temperature T_t was 127.7°F, and the data at the right were obtained at a cryogenic temperature of $-271.4°$F. It should be mentioned that the tunnel stagnation temperature T_t used in the reduction of data is measured with a refined, individual, temperature sensor located just upstream of the temperature survey ring toward the turning vanes. (See small insert sketch in Fig. 5.) The symbols included with the sketch of the survey ring indicate the locations of the various measurements shown in the temperature distribution plots. The temperature plots indicate the temperature variations across the calibration ring. In both cases, it was slightly warmer near the walls of the tunnel with a standard deviation σ (measure of dispersion around the mean) of only about 1°F at both the cryogenic and ambient stagnation temperatures.

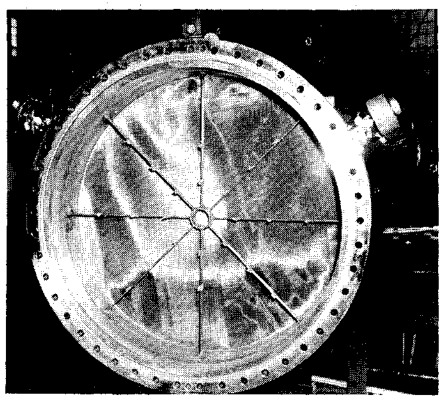

Fig. 4 Temperature survey ring installed in screen section of tunnel.

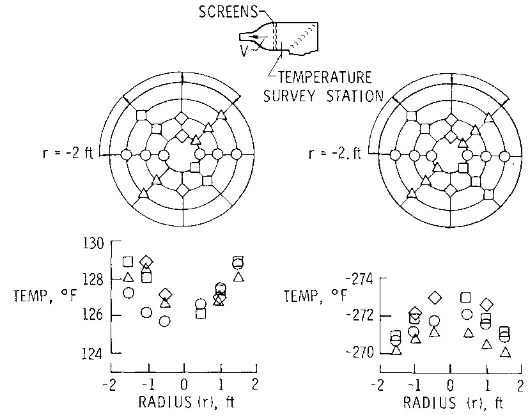

Fig. 5 Temperature distributions in screen section. $M_\infty = 0.85$, $P_T = 5$ atm.

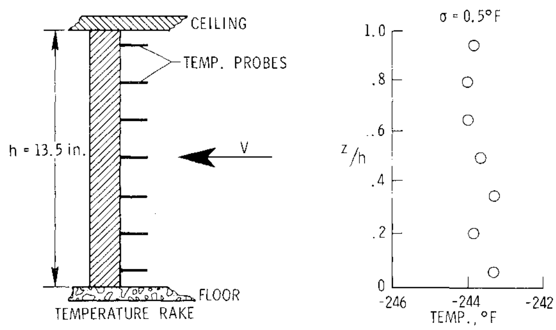

Fig. 6 Temperature distribution in test section. $M_\infty = 0.85$, $P_T = 5$ atm.

Since the survey ring was located upstream of the smoothing screens and contraction section (see sketch, Fig. 5), it might be expected that a more uniform distribution would occur in the test section than at the survey ring. This did prove to be the case. Of ultimate concern, of course, is the temperature distribution of the test gas in the test section. A temperature survey rake was used which could be oriented across the test section in vertical, horizontal, or lateral positions. The rake consisted of seven evenly spaced thermocouple probes which protruded from a streamlined strut support.

An example of test-section temperature distributions which were determined at Mach 0.85 at a near-maximum stagnation pressure and a cryogenic stagnation temperature is shown at the right of Fig. 6. These results show the temperatures which were determined at the various probe positions. The results show the excellent distribution which was obtained at a cryogenic temperature of $-243.7°$F. (Standard deviation σ was 0.5°F.) When test-section temperature distributions were taken at the very beginning of a series of tests, that is, just af-

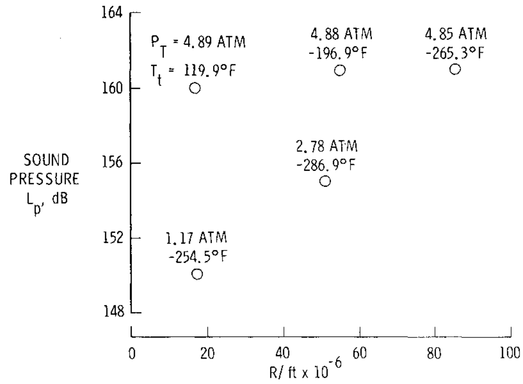

Fig. 7 Test-section sound pressure levels adjacent to a model at angle of attack. $M_\infty = 0.80$.

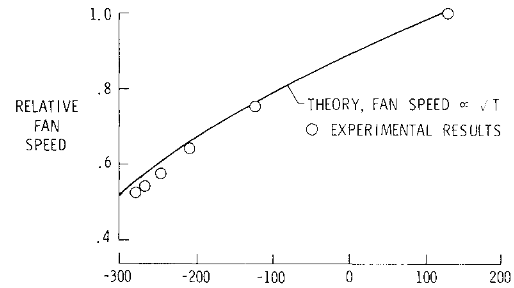

Fig. 8 Theoretical and experimental fan speeds at $M_\infty = 0.85$, $P_T = 4.95$ atm.

ter tunnel "cool down" there was a moderate peak in the distributions, indicating slightly warmer temperatures near the test-section walls and plenum chamber. This trend disappeared rapidly but it was very similar to the behavior of the distributions determined with the survey ring in the screen section of the tunnel.

The temperature studies have shown remarkably good distributions. This is particularly obvious in view of the fact that it is not uncommon for conventional ambient temperature wind tunnels to have temperature gradients of over 20°F in the test section. These encouraging results indicate that cooling by injecting liquid nitrogen directly into the tunnel circuit is practical at the power levels required for transonic testing, and that good temperature distribution can be obtained by using a simple liquid nitrogen injection system.

Noise Level Measurements

In wind-tunnel testing, background noise in the test section is of concern since excessive noise levels can obstruct the proper simulation of unsteady aerodynamic parameters ususally of interest in dynamic tests. In addition, test-section noise can affect angle-of-attack measurements, boundary-layer transition, and certain static or steady-state parameters. Because of the large reductions in drive power as temperature is reduced, it was expected that background noise would be reduced when a given Reynolds number was obtained at cryogenic temperatures rather than at ambient temperature. A preliminary study was made to check this hypothesis.

The results presented in Fig. 7 show some trends that were obtained with a microphone located in the test section. Sound pressure level L_p in decibels is plotted against Reynolds number per foot at a constant Mach number 0.80 for various pressure and temperature conditions. The noise levels are presented in terms of the broadband (10 Hz-20 Hz) sound pressure level, with the reference pressure taken to be 2.9 × 10^{-9} lbs per square inch. These measurements were made during the testing of a two-dimensional airfoil at an angle of attack of 3°. The results, therefore, do not represent a pure indication of the minimum background noise and should only be used as comparative levels to indicate the general effects of changes in pressure and temperature. In Fig. 7, the tunnel conditions (stagnation pressure and temperature) at which the noise measurements were taken are shown adjacent to each of the plotted points. It will be noted that at constant Reynolds number of about 19 × 10^6 per ft operating at a temperature of —254.5°F allowed the desired Reynolds number to be obtained at the lower pressure of 1.17 atm and reduced the sound pressure level by 10 db.

The results shown across the upper portion of Fig. 7 indicate that by reducing the tunnel temperature to −265.3°F at a constant pressure of about 4.9 atm, the Reynolds number is increased by a factor of 4.6 with only a 1db increase in noise level. It might be expected that a reduction in noise level would occur at the higher stagnation pressures when the tunnel was operated at cryogenic temperatures due to the reduced power requirements (see Fig. 1). Although the slight increase in level is not completely understood, it is believed to be associated with an increase in noise arising from the increased rate of nitrogen being exhausted from the tunnel at the cryogenic temperatures. If this is the case, special attention to the design of the nitrogen exhaust systems could very possibly result in additional noise reductions at all operating conditions.

An extensive analysis of test-section noise has not been made, however, these limited results have indicated some promising trends. It appears that with regard to tunnel noise level, the primary advantage of operating at cryogenic temperatures is the ability to obtain a given Reynolds number at a lower stagnation pressure and thereby with a lower sound pressure level.

Experimental and Theoretical Drive Power and Fan-Speed Studies

During the initial calibrations and aerodynamic testing, measurements were made of both the drive-shaft torque and fan speed to permit comparisons with theoretical predictions at various conditions of temperature, pressure, and Mach number. At this time, the drive-power results have not been completely evaluated. However, from preliminary data based on power supplied to the drive motor, it appears that drive power varies roughly as predicted, that is, for constant pressure and Mach number, power varies directly with the speed of sound, or as $\sqrt{T}$.

A sufficient number of fan-speed measurements have been made to evaluate the agreement between theory and experimental results. Figure 8 shows the theoretical and experimental variation of fan speed with temperature at a constant Mach number of 0.85 and at a constant stagnation pressure of about 4.95 atm. The Reynolds numbers varied from about 19 × 10^6 per ft at the highest temperature to 100 × 10^6 per ft at the lowest cryogenic temperature condition. The experimental results, shown by the circular symbols, indicate that the fan speed actually decreases somewhat faster than predicted by simple theory (speed $\propto \sqrt{T}$). Thus, at cryogenic temperatures the greatly increased Reynolds number has, as would be expected, a beneficial effect on tunnel performance and/or fan efficiency.

Two-Dimensional Airfoil Study

As noted in Ref. 3, the theoretical real-gas studies which have been made at the Langley Research Center indicate that for moderate operating pressures the flow characteristics are insignificantly affected by the real-gas "imperfections" of nitrogen at cryogenic temperatures. Shortly after the initial tunnel calibrations, a series of two-dimensional airfoil tests were conducted to provide experimental confirmation of the cryogenic concept and the validity of the theoretical studies. The configuration selected for these studies was a 12% thick, NACA 64-series airfoil equipped with pressure orifices. A photograph of the model is shown in Fig. 9. The 5.4-in. airfoil completely spanned the 13.5-in. test section. The sketch shown at the lower left of the figure indicated that at subcritical speeds, the 64-series airfoils have a "flat top" velocity distribution, similar to the upper surface distribution of current supercritical designs.

There were several conditions which were selected to assure an adequate cryogenic evaluation: 1) tests at ambient and cryogenic temperatures were to be made in the same tunnel, on the same model, at identical Mach numbers and Reynolds numbers; 2) the airfoil was to be tested with free transition to allow any possible temperature effect on boundary-layer development; 3) the symmetrical airfoil was to be tested at a lift coefficient of zero to eliminate any shape or angle-of-attack change due to dynamic pressure differences; and 4) the test Mach number would exceed the leading-edge Mach number of typical sonic transport designs.

Figure 10 illustrates the operating envelope considered in the two-dimensional airfoil studies. Stagnation pressure P_T is plotted against unit Reynolds number as well as Reynolds number based on model chord. The operating envelope is bounded by the stagnation pressure limits (horizontal lines) and stagnation temperature limits (diagonal curves). The curves for the theoretical saturation limits associated with the local and freestream Mach numbers are indicated. The circular symbols illustrate the conditions for tests performed at $M_\infty = 0.85$ and Reynolds numbers ranging from about 4.5×10^6 to 100×10^6 per ft. In the following paragraphs, pressure distributions that were obtained on the two-dimensional airfoil at $M_\infty = 0.85$ will be discussed. The test conditions for these distributions are shown on this envelope as the solid symbols.

Figure 11 shows a comparision of the upper surface pressure distributions obtained at identical Reynolds numbers at both ambient and cryogenic temperatures for freestream Mach numbers of 0.75 and 0.85. The circular symbols indicate pressure coefficients obtained at a stagnation pressure of about 4.9 atm and at ambient temperature. The square symbols indicate pressure coefficients obtained at about 1.2 atm and at a cryogenic temperature of $-250°$F.

Several types of flowphenomena are illustrated in Fig. 11. The results for $M_\infty = 0.75$ are unmistakably subcritical. The results for $M_\infty = 0.85$ indicates that the local Mach number becomes sonic (at $C_p = -0.3$) and continued to increase until a strong recompression shock was produced. In both cases, there is excellent agreement between the results for cryogenic and ambient temperatures. This agreement was achieved despite the sensitivity of the airfoil to changes in Mach number and the large variation in the speed of sound at the two temperatures. These results clearly demonstrate the ability to set the tunnel conditions accurately and substantiate the theoretical findings that cryogenic gaseous nitrogen is a valid test medium.

Figure 12 shows an example of the studies which were made to examine the effects of operating at the theoretical saturation boundaries. The variations of pressure coefficients are shown for two different pressure and temperature conditions at a constant Reynolds number of 27×10^6. The circular symbols are the results obtained at $-210.2°$F, well above either the local or freestream saturation boundary. The square symbols are the results obtained at a stagnation temperature which resulted in the saturation boundary just being reached at freestream conditions. The excellent agreement between the results suggests that additional Reynolds number capabilities can be expected from the cryogenic wind tunnel by testing at temperatures approaching the theoretical freestream saturation boundary.

The two-dimensional airfoil tests substantiated that cryogenic test conditions can be set accurately and that gaseous nitrogen is a valid transonic test medium which allows the achievement of high Reynolds numbers without increases in aerodynamic loading. In addition, this particular

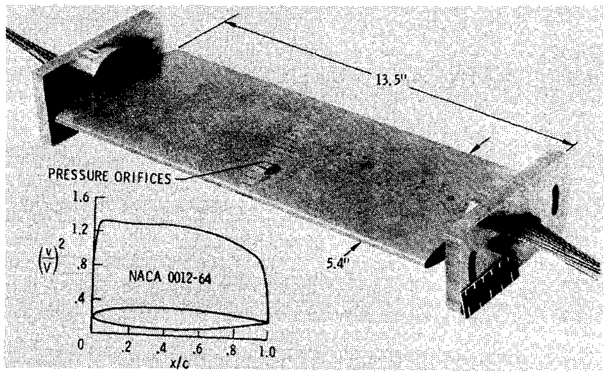

Fig. 9 Proof of concept, two-dimensional airfoil model.

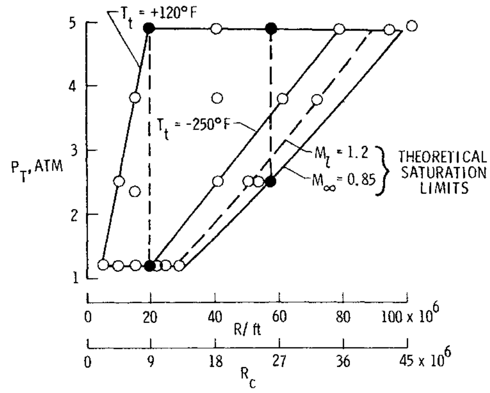

Fig. 10 Test conditions for two-dimensional airfoil at $M_\infty = 0.85$.

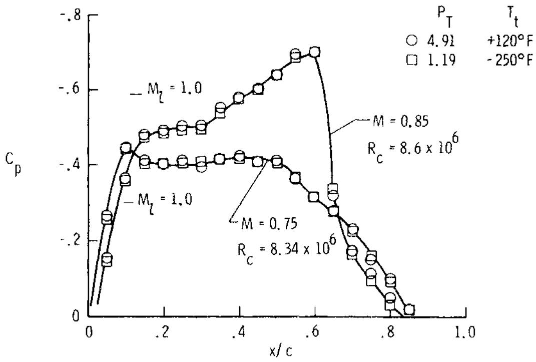

Fig. 11 Pressure distributions on two-dimensional airfoil at ambient and cryogenic conditions. $\alpha = 0°$.

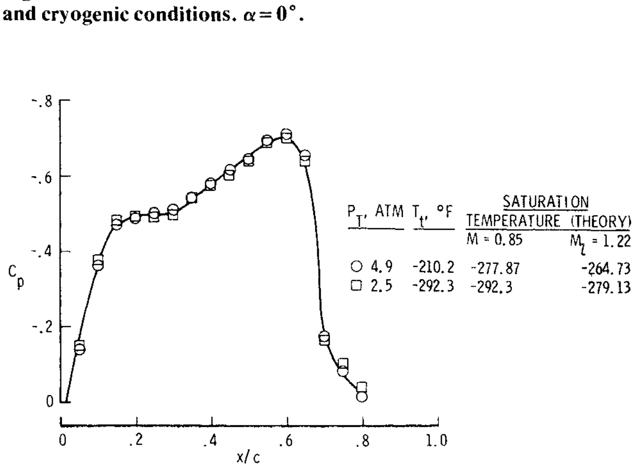

Fig. 12 Two-dimensional pressure distributions indicating the effects of operating at the theoretical saturation limit $M_\infty = 0.85$, $\alpha = 0°$, $R_c = 27 \times 10^6$.

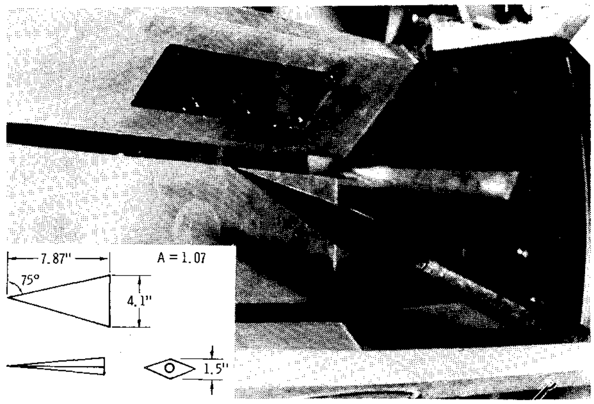

Fig. 13 Three-dimensional delta-wing model installed in the test section.

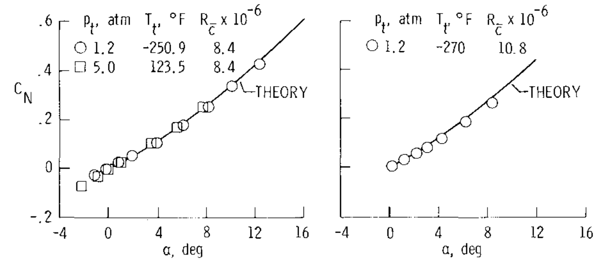

Fig. 14 Normal force coefficients determined for the three-dimensional model at ambient and cryogenic temperatures. Curve on right is for $M_\infty = 1.10$ and curve on left is for 0.85.

series of studies indicated that substantial additional increases in Reynolds number capability may be realized by testing beyond the theoretical local saturation boundary.

Three-Dimensional Model Tests

Three-dimensional model tests have been made in the transonic cryogenic tunnel using a sharp leading-edge delta wing having an aspect ratio of 1.07 and a sweep of 75°. A sketch and photograph of the model are shown in Fig. 13.

The purposes of the three-dimensional model tests were: 1) to investigate any possible effects of cryogenic conditions on the aerodynamic characteristics of a configuration having flow characterized by a separation induced leading-edge vortex; and 2) to obtain cryogenic experience with an electrically-heated strain-gage balance and the accompanying sting, a strut, and angle-of-attack measuring devices. (Similar tests had been made previously in Langley's low-speed cryogenic tunnel using a water-heated balance with satisfactory results.[2])

With regard to the current studies in the transonic cryogenic tunnel, the preliminary results were encouraging. Some problems have been encountered with respect to balance zero shifts, however, the three-component balance results show that angle-of-attack effects are duplicated at ambient and cryogenic temperatures and that electrically-heated balances, as well as the previously studied water-heated balances, are feasible for cryogenic operation. In addition, there are no fundamental problems associated with measuring angle of attack at cryogenic temperatures and the pitching moment, axial force, and normal force results indicate that leading-edge vortex type flows are duplicated properly at cryogenic temperatures. An example of the angle-of-attack effects are shown in Fig. 14 which shows the variation of normal force coefficient with angle of attack at Mach numbers of 0.85 and 1.1. Although the primary purpose of this phase of the study was to obtain comparisons between ambient and cryogenic temperature results, theoretical predictions of normal force by the method of Ref. 4 have been included with the experimental results (see solid lines.) These predictions were included in this presentation to provide a basis for comparison at $M_\infty = 1.1$ since at this Mach number, the increased aerodynamic loadings required to obtain experimental data at ambient temperature would have resulted in forces and moments exceeding the limits of the strain-gage balance system. At $M_\infty = 0.85$, the circular symbols indicate experimental results obtained at a stagnation pressure of 1.2 atm and at a cryogenic temperature of about −250°F. The results represented by the square symbols were taken at a stagnation pressure of 5 atm and at a temperature of 123.5°F. The Reynolds number, based on model geometric chord, was $8{,}4 \times 10^6$ for both sets of data. As can be seen, there is good agreement between theory and the experimental results obtained at both the ambient and cryogenic temperatures. At the right of the figure, the cryogenic results for $M_\infty = 1.1$ are presented and compared with theory and the results appear to also confirm that there are no extraneous temperature effects. The small differences are not surprising since experience has indicated that at supersonic speeds there is generally good agreement with theory at low angles of attack and that the theory predicts slightly more vortex lift than is actually produced at the higher angles of attack.

The three-dimensional model results have provided additional evidence that cryogenic nitrogen is a valid test gas even under conditions of separated and reattached (vortex) flow. In addition, there has been no indication of any major problem areas associated with obtaining angle-of-attack or strain-gage balance measurements at cryogenic temperatures.

Conclusions

The Langley pilot transonic cryogenic tunnel has recently been developed. Validation tests of this tunnel have led to the following conclusions. 1) The cryogenic approach offers a feasible method for acquiring transonic test results at high Reynolds number and at reduced levels of dynamic pressure and tunnel drive power. 2) With the unique ability to control tunnel temperature, pressure, and Mach number separately, it is possible to determine independently the effects of Reynolds number, dynamic pressure and compressibility on the aerodynamic characteristics of the model under test. 3) Cooling with liquid nitrogen is practical at the power levels required for transonic testing. Test temperature is easily controlled and good tempeature distribution obtained by using a simple nitrogen injection system. 4) Test-section noise level is reduced when a given Reynolds number is obtained by operating at cryogenic temperatures. 5) Two-dimensional and three-dimensional model tests have provided additional substantiation that cryogenic test conditions can be set accurately and that cryogenic gaseous nitrogen is a valid test medium. 6) Testing at temperatures several degrees beyond the local supersaturation boundary have been accomplished with no detectable effect on the pressure distribution over a two-dimensional airfoil.

References

[1] Smelt, R., "Power Economy in High-Speed Wind Tunnels by Choice of Working Fluid and Temperature," Rept. Aero. 2081, Aug. 1945, Royal Aircraft Establishment, Farnborough, England.

[2] Goodyear, M. J. and Kilgore, R. A., "High Reynolds Number Cryogenic Wind Tunnel," *AIAA Journal*, Vol. 11, May 1973, pp. 613-619.

[3] Kilgore, R. A., Adcock, J. B., and Ray, E. J., "Simulation of Flight Test Conditions in the Langley Pilot Transonic Cryogenic Tunnel," TN D-7811, Dec. 1974, NASA.

[4] Polhamus, E. C., "Charts for Predicting the Subsonic Vortex-Lift Characteristics of Arrow, Delta, and Diamond Wings," TN D-6243, April 1971, NASA.